ANALYSIS OF 2D PHOTONIC CRYSTAL CAVITIES USING A MULTI-SCATTERING APPROACH BASED ON WEIGHTED BESSEL FUNCTIONS

H. Abiri, R. Ghayour, and M. Mahzoon

Electrical Engineering Department
Shiraz University
Shiraz, Iran

Abstract—A semi-analytic method, based on scattering approach is applied to analyze the finite size photonic crystal cavities surrounded by cylindrical dielectric rods. The resonant frequency and the quality factor (Q) are determined by this method. Also, with a source at the center of the cavity, field and energy distribution can be obtained at different frequencies. The algorithm is simple to simulate on PCs. There is no need for absorbing boundary conditions which are required in most numerical methods. Using the symmetry of the structure the computational cost is reduced to 1/8 and 1/12 those of the square and hexagonal lattices respectively. Since the computational time is very low (in the order of one minute) the variation in size and dielectric constant of the rods can be examined easily. It is shown as an example that by varying the radius of the rods according to their distance from the center of the cavity, the Q factor is increased considerably in comparison with that of uniform structures.

1. INTRODUCTION

In recent years, photonic crystals have gained much attention for their many fascinating properties. Among them, the more interesting ones are localizing the light in resonant cavities [1], ability to guide light beam even through a sharp bend [2], etc. Most of the properties are based on the ability of photonic crystals in exhibiting a complete photonic band gap, where light within that band gap cannot propagate through the crystal in any direction [3]. Generally, resonant cavities are formed by introducing point defects in the periodic lattice. These structures exhibit localized modes in the bandgap region with a very

narrow spectra and high Q factor in a small area, becoming a good candidate for laser fabrication [4].

Different numerical methods have been used to study the localized modes in photonic crystal cavities. The well known methods are; plane-wave-expansion method (PWM) [4], finite-difference-time-domain analysis (FDTD) [5, 6], finite-element method (FEM) [7–9], scattering matrix method (SMM) [10–12] and Wannier equation method [13]. In PWM and Wannier equation methods, a super-cell with the periodic defects is considered. On the other hand, in numerical methods such as FEM, one cell is considered to be analyzed and the absorbing boundary conditions must be considered around the cell for justifying the boundary conditions. The method presented in this paper is a semi-analytical method based on multi- scattering approach in cylindrical coordinates.

The SMM is applied to 2D photonic crystals consisting of the cylindrical dielectric rods. The theory is based on the fact that: the total field around each cylindrical dielectric rod in photonic crystals contains two main components, i) the total incident field and ii) the field scattered by that cylinder itself.

The total incident field in turn consists of two parts a) the field due to the external source and b) the field due to the total scattering from all the other rods that are incident to the cylinder under consideration. The analytical expressions for determining the field at any point within the photonic crystal can be obtained by relating the field scattered from each dielectric cylinder to the field incident to it. For numerical analysis, we assume that the incident field of part (b), around each cylinder, is in the form of a Fourier-Bessel series with finite number of terms and unknown coefficients. Therefore, the scattered field from the rods can be determined analytically in terms of the unknown coefficients. Now, the incident field at any point near each rod must be equal to the sum of the entire scattered fields from the other rods plus the fields from the external source at that point. By applying this scheme at a sufficient number of points around the rods, the unknown coefficients of the Fourier-Bessel series and hence the total field inside the structure can be determined.

The algorithm for this method is simple and efficient as far as CPU capacity and computational time are concerned. Application of symmetry reduces the volume of computation significantly, e.g., in square lattices, 1/8 of the structure and for hexagonal lattices only 1/12 of the structure is enough to be calculated. Thus, we can simply compare the properties of the cavity for different parameters such as the radius of rods, the lattice constant and the dielectric constant. Also, the field and energy distribution can be obtained at different

wavelengths of the incident light without spending too much time.

2. THEORY

As mentioned before when a number of dielectric cylinders are illuminated by an external light source, it is possible to define, in the vicinity of the surface of each cylinder, two complementary parts of the field: i) the total incident field and, ii) the field scattered by that cylinder. Meanwhile, the total incident field in turn consists of two components: The field due to the external source denoted by $\mathbf{E^{ex}}$ and the field due to the scattering from other cylinders denoted by $\mathbf{E^i}$. Therefore, at any point in the vicinity around the rod number m we can write:

$$\mathbf{E}_m^i = \sum_{k=1,k\neq m}^{N} \mathbf{E}_k^s, \quad m = 1, 2, \ldots, N \tag{1}$$

where N is the total number of rods, $\mathbf{E}_m^i$ is the field incident to the rod number m due to the scattering from all other rods and $\mathbf{E}_k^s$ is the scattered field coming from the rod number k. The mechanism is shown in Fig. 1 for three cylindrical obstacles. From the figure it is clear that the total incident field to each rod is equal to the sum of the fields scattered by the other two rods plus the incident field originating from the external source.
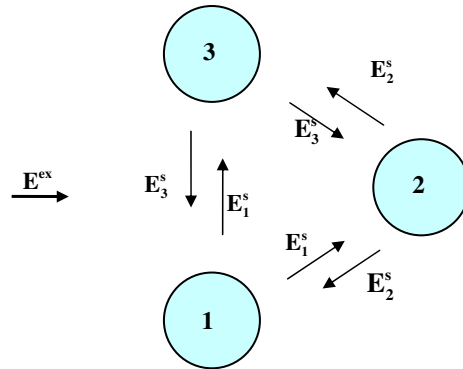
Figure 1. Demonstration of multiple scattering between three obstacles illuminated by an external source.

On the other hand, the scattered field from rod number k is in turn a function of the total incident field to this rod. That is:

$$\mathbf{E}_k^s = F\left[\mathbf{E^{ex}} + \mathbf{E}_k^i\right] \tag{2}$$

where $\mathbf{E^{ex}}$ and $\mathbf{E_k^i}$ are the fields incident to the rod number k from the external source and multi-scattering respectively. In the case of a cylindrical wave incident to a dielectric cylindrical rod, the function F in (2) is an analytic function and is derived later as expressed in (9) and (10). Substituting (2) in (1) gives:

$$\mathbf{E_m^i} = \sum_{k=1, k \neq m}^{N} F\left[\mathbf{E^{ex}} + \mathbf{E_k^i}\right], \quad m = 1, 2, \ldots, N \tag{3}$$

This is a system of equations that relates the unknown incident fields to the known source field and is used as the basis of the system of equations for determining the field distribution within the photonic crystal. To solve (3), the following technique is used:

The source is assumed to be a 2-D cylindrical source, with angular frequency ω and amplitude I, located at the center of the cavity. Thus, the radiated electric field is in the form of Hankel function of the second kind. In other words, the incident field due to the external source, at an arbitrary point $\mathbf{n}(r_n, \varphi_n)$ around the rod number k, can be expressed as follows [14]:

$$\mathbf{E^{ex}}(r_n, \varphi_n) = \mathbf{a_z} \frac{-\mu_0 I}{4} \omega H_0^{(2)}(\beta_0 r_n) \tag{4}$$

where (r_n, φ_n) denotes the polar coordinate of a point $\mathbf{n}$ when the origin of the coordinates is located at the center of the cavity. The scattered field by each dielectric rod, due to the above incident field, can be determined analytically. First, by the Graf's addition theorem, we transform the Hankel function given in (4) to the center of the rod under consideration. Thus, referring to Fig. 2 for rod k and point $\mathbf{n}$, we can write:

$$H_0^{(2)}(\beta_0 r_n) = \sum_{p=-\infty}^{\infty} H_p^{(2)}(\beta_0 ro_k) J_p(\beta_0 r_{nk}) \exp(-jp\theta_{nk}), \quad r_{nk} < ro_k \tag{5}$$

where $\theta_{nk} = \pi - (\varphi_{nk} - \varphi o_k)$, (r_{nk}, φ_{nk}) is the coordinate of point $\mathbf{n}$ with respect to the center of the rod k(denoted by $\mathbf{O}_k$), and $(ro_k, \varphi o_k)$ the coordinate of $\mathbf{O}_k$ with respect to the center of the cavity. Similar notations may be assigned to other points and rods. For example, (r_m, φ_m) represents the coordinate of the point $\mathbf{m}$ with respect to the center of the cavity and (r_{mq}, φ_{mq}) shows the coordinate of the point $\mathbf{m}$ with respect to the center of the rod no. q. Also $\mathbf{O}_q(ro_q, \varphi o_q)$ shows the center of the rod no. q with respect to the center of the cavity.

Using (4) and (5), the incident field due to the external source, in the vicinity of the rod no. k, may be expressed as follows:
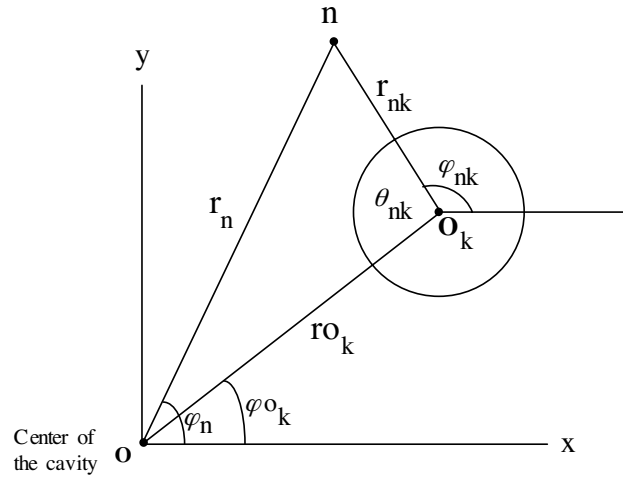
Figure 2. Illustration of two polar systems located at the center of the cavity and the center of rod k. The coordinates of a point $\mathbf{n}$ in both systems are shown.

$$E^{ex}(r_{nk}, \varphi_{nk})$$
$$= \sum_{p=-\infty}^{\infty} \left[\frac{-\mu_0 I}{4} \omega \exp(-jp(\pi + \varphi o_k)) H_p^{(2)}(\beta_0 r o_k) \right] J_p(\beta_0 r_{nk}) \exp(jp\varphi_{nk})$$
$$= \sum_{p=-\infty}^{\infty} A_{pk}^{ex} J_p(\beta_0 r_{nk}) \exp(jp\varphi_{nk}) \tag{6}$$

where the term in bracket denoted by A_{pk}^{ex} is a constant depending on the position of rod no. k. Since the field is assumed to be **TM** to $\mathbf{z}$ in the structure, the electric field is in the $\mathbf{z}$ direction at all the points. Thus, Equation (6) and the following equations are expressed in scalar form and E in these equations, represents the $\mathbf{z}$ component of the electric field. The field due to the external source incident to the other rods can also be represented as a summation of Bessel functions similar to those in (4). The scattered fields, due to these incident fields, are in the form of Hankel functions [14]. As a result, the field incident to rod no. k due to scattering from the other rods is in the form of Bessel functions with respect to the center of that rod and can be written as follows:

$$E_k^i(r_{nk}, \varphi_{nk}) = \sum_{p=-\infty}^{\infty} A_{pk}^i J_p(\beta_0 r_{nk}) \exp(jp\varphi_{nk}) \tag{7}$$

where $A_{pk}^i{}'s$ are unknown coefficients that must be determined. The total field incident to rod no. k, at an arbitrary point $\mathbf{n}(r_n, \varphi_n)$, is:

$$E^{ex}(r_n, \varphi_n) + E_k^i(r_n, \varphi_n) = \sum_{p=-\infty}^{\infty} \left[A_{pk}^{ex} + A_{pk}^i \right] J_p(\beta_0 r_{nk}) \exp(jp\varphi_{nk}) \quad (8)$$

and the total scattered field from rod no. k is:

$$E_k^s(r_n, \varphi_n) = \sum_{p=-\infty}^{\infty} a_p \left[A_{pk}^{ex} + A_{pk}^i \right] H_p^{(2)}(\beta_0 r_{nk}) \exp(jp\varphi_{nk}) \quad (9)$$

where [14]:

$$a_p = j^{-p} \frac{J_p'(\beta_0 b) J_p(\beta_1 b) - \sqrt{\varepsilon_r} J_p(\beta_0 b) J_p'(\beta_1 b)}{\sqrt{\varepsilon_r} J_p'(\beta_1 b) H_p^{(2)}(\beta_0 b) - J_p(\beta_1 b) H_p^{(2)'}(\beta_0 b)} \quad (10)$$

where b is the radius, ε_r the dielectric constant and β_1 the wave constant in the rods respectively.

Substituting (7) and (9) in (3), the following expression is resulted:

$$E_m^s(r_n, \varphi_n) = \sum_{p=-\infty}^{\infty} A_{pm}^i J_p(\beta_0 r_{nm}) \exp(jp\varphi_{nm})$$

$$= \sum_{k=1, k \neq m}^{N} \left[\sum_{p=-\infty}^{\infty} a_p (A_{pk}^{ex} + A_{pk}^i) H_p^{(2)}(\beta_0 r_{nk}) \exp(jp\varphi_{nk}) \right] \quad (11)$$

where N is the total number of rods in the structure, as defined in (1). To solve (11), we truncate the second summation to P. Then the number of unknowns A_{pk}^i will be $N(2P+1)$. Thus (11) must be written at $N(2P+1)$ points in the structure around all the rods, i.e., $(2P+1)$ points around each rod. Rearranging (11), we obtain a system of linear equations as follows:

$$\sum_{p=-P}^{P} \sum_{k=1}^{N} B_{pk}(\beta_0 r_{nk}) \exp(jp\varphi_{nk}) A_{pk}^i =$$

$$\sum_{k=1, k \neq m}^{N} \left[\sum_{p=-P}^{P} a_p A_{pk}^{ex} H_p^{(2)}(\beta_0 r_{nk}) \exp(jp\varphi_{nk}) \right] \quad (12)$$

where $B_{pm} = J_p$ for $k = m$; $B_{pk} = -a_p H_p^{(2)}$ for $k \neq m$; $n = 1, 2, \ldots, N(2P+1)$. In matrix form, Equation (12) can be represented as:

$$\mathbf{M A^i = N A^{ex}} \quad (13)$$

where $\mathbf{A^i}$ is the unknown column vector with $N(2P+1)$ elements, $\mathbf{A^{ex}}$ is a vector defined in (6) and $\mathbf{M}$ and $\mathbf{N}$ are square matrices with dimension $N(2P+1) \times N(2P+1)$; their elements are described in (12).

Due to symmetry in real structures (photonic crystals), the fields around the similar rods are alike and in most of the practical cases, the number of unknowns in (12) is quite less than $N(2P+1)$.

Obtaining the coefficients $\mathbf{A^i}$, field distribution in the structure can be determined. The field outside each dielectric rod is given by (9) and (10). Also, the diffracted field (field inside the rods) can be obtained from the total incident field to each rod, and the result is:

$$E_k^d(\mathbf{n}) = \sum_{p=-\infty}^{\infty} c_p \left[A_{pk}^{ex} + A_{pk}^i \right] J_p(\beta_1 r_{nk}) \exp(jp\varphi_{nk}) \qquad (14)$$

where point $\mathbf{n}(r_n, \varphi_n)$ is assumed to be inside the dielectric rod no. k, and c_p is given by [14]:

$$c_p = j^{-p} \frac{J_p(\beta_0 b) H_p^{(2)'}(\beta_0 b) - J_p'(\beta_0 b) H_p^{(2)}(\beta_0 b)}{J_p(\beta_1 b) H_p^{(2)'}(\beta_0 b) - \sqrt{\varepsilon_r} J_p'(\beta_1 b) H_p^{2}(\beta_0 b)} \qquad (15)$$

where b, ε_r and β_1 are as defined in (10).

3. NUMERICAL RESULTS

The method is used to analyze the square and hexagonal lattices of cylindrical rods with cavities at the center. The results are focused on the field distribution and quality factor and are compared with the results of other methods. Each of these cavities is formed by removing the central rod from the center of the lattice as shown in Fig. 3. The specifications of the structures are chosen similar to those in [9] for the purpose of comparison.

3.1. Square Cavity

This cavity consists of an $n \times n$ array of dielectric rods with lattice constant a, embedded in air, where the central rod is removed. The dielectric constant of rods ε_r is equal to 11.56 and their radius r is equal to $0.2a$. For resonance to occur at $\lambda = 1.55$ microns, the lattice constant a is chosen as 0.58652 microns.

The number of terms in series (7) is taken equal to 15. Increasing this number does not affect the solutions noticeably. By symmetry, only 1/8 of the domain of square lattice leads to a complete solution.
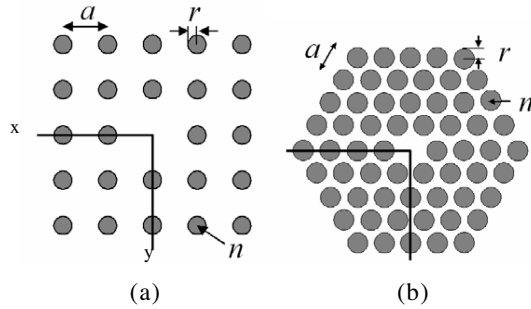
Figure 3. Structure of 2-D photonic crystal cavities with (a) square lattice and (b) hexagonal lattice.
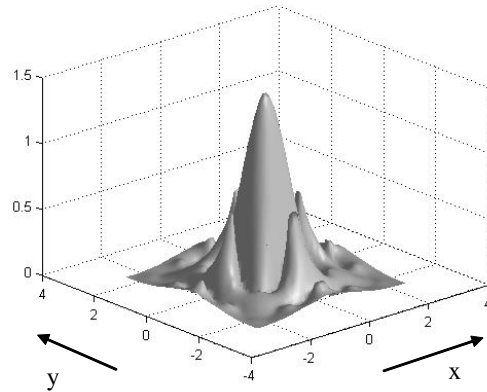
Figure 4. Field distribution in a 5 by 5 square cavity at resonance.

Thus, for a 5×5 square cavity, which contains 24 rods, the total number of unknown coefficients is 47. This is equal to 93 for a 7×7 structure and equal to 154 for a 9×9 cavity. As a result, the number of equations in (13) is very low and the computation time is less than one minute on a common PC. The electric field distribution in a typical 5×5 square cavity at resonant frequency is calculated and plotted in Fig. 4. This is similar to the results obtained using finite-element method [9]. The Q factors of three different sizes of the structure; 5×5, 7×7 and 9×9 are determined by monitoring the field amplitude at different frequencies. The results are shown in Table 1, and compared with the results of finite element (FE) [9]. The variation of the energy within a 5×5 square cavity versus frequency is shown in Fig. 5. It is noticeable that increasing the size of the crystal increases the quality factor significantly and does not tend to a limit. The reason for such a
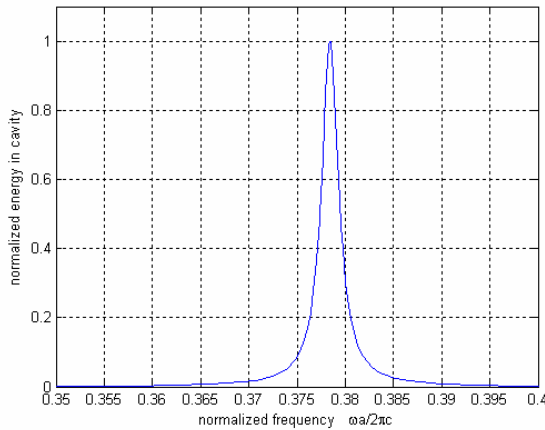
Figure 5. Energy spectra in the square cavity versus the normalized frequency.

nonphysical unlimited Q factor is in fact, infinite length of the rods. In [15, 16], it is shown that the use of a photonic double hetero-structure can prevent reduction of Q-factor due to the limited height.

Table 1. Values of Q factor for square cavity.

size	Scattering Method	FE
5×5	178	178
7×7	1390	1414
9×9	9930	10276

Modification of the structure can easily be studied. For example, by adjusting the radius of the rods according to their distance from the center of the cavity, the Q factor can be changed. For the structure shown in Fig. 6, the angle looking at the rods are constant and in addition, the average area of the rods cross sections is $\pi(0.2a)^2$. The calculated Q factor is increased to 605 which is more than three times greater compared to Q of the same structure with identical rods of radius $0.2a$.
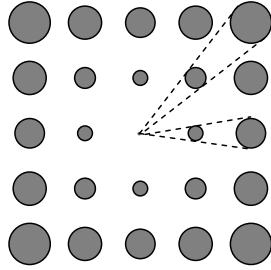
Figure 6. Structure of inhomogeneous 2-D square cavity. The angles looking the rods are the same.
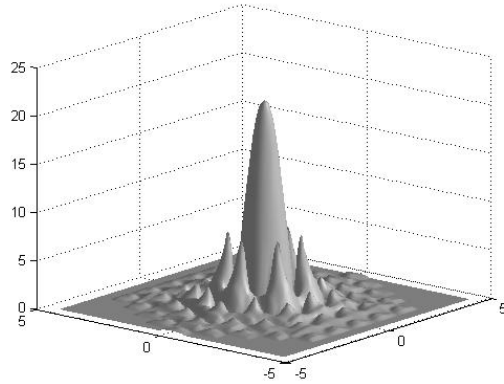
Figure 7. Field distribution in a 4-ring hexagonal cavity at resonance.

3.2. Hexagonal Cavity

Four-ring, five-ring and six-ring hexagonal lattices of cylindrical rods with the cavities at the centers are analyzed by this method. The dielectric constant of the rods ε_r is equal to 9 and the radius r is equal to $0.378a$. The lattice constant a is chosen as 0.7254 microns to obtain resonance frequency at λ of 1.55 microns.

Applying the symmetry of the structure and choosing 15 unknown coefficients for the incident wave to each rod, the total number of unknowns is 78 for four-ring, 116 for five-ring and 162 for six-ring hexagonal cavity. Field distribution for four-ring cavity is shown in Fig. 7 and the Q factors of three different structures are given in Table 2. The results are in correlation with the results obtained by finite-element analysis [9].

Again modification of the radii may increase the Q factor; e.g., reducing the radius of the rods around the center of the cavity to half, increases the Q factor of the four-ring cavity to 2650.

Table 2. Values of Q factor for hexagonal cavity.

size	Scattering Method	FE
4 rings	1771	1745
5 rings	18150	18081
6 rings	182030	- - -

4. CONCLUSION

The semi-analytic method presented in this paper is efficient and accurate, while the computational efforts and consuming time are very low. It is applicable to 2-D structures having cylindrical rods. The number of unknowns (i.e., the number of terms in Fourier-Bessel series) which must be chosen for an accurate analysis may be quite low. There is no error due to the numerical techniques such as mesh generation and absorbing boundary condition. The method is applied to the 2-D cavities with cylindrical dielectric rods with different sizes and structures. In spite of low computational effort and time, the results of this approach are in very good correlations with the results of other numerical methods.

Because of the low computational time (order of one minute), modified cylindrical structures can also be analyzed simply. The effect of variation in the radius of each group of cylinders on the Q factor is demonstrated.

REFERENCES

1. John, S., "Strong localization of photons in certain disordered dielectric superlattices," *Phys. Rev. Lett.*, Vol. 58, 2486–2489, June 1987.
2. Mekis, A., J. C. Chen, I. Kurland, S. Fun, P. R. Villeneuve, and J. D. Joannopoulos, "High transmission through sharp bends in photonic crystal waveguides," *Phys. Rev. Lett.*, Vol. 77, No. 18, 3787–3790, Oct. 1996.
3. Yablonovitch, E., "Inhibited spontaneous emission in solid-state physics and electronics," *Phys. Rev. Lett.*, Vol. 58, 2059–2062, May 1987.
4. Joannopoulos, J. D., R. D. Meade, and J. N. Winn, *Photonic*

Crystals: Molding the Flow of Light, Ch. 7, Princeton University Press, Princeton, NJ, 1995.

5. Sakoda, K., *Optical Properties of Photonic Crystals*, Ch. 6, Springer-Verlag, New York, 2001.

6. Sakoda, K., "Numerical study on localized defect modes in two-dimensional triangular photonic crystals," *J. Appl. Phys.*, Vol. 84, 1210–1214, Aug. 1998.

7. Hwang, J. K., S. B. Hyun, H. Y. Ryu, and Y. H. Lee, "Resonant modes of two-dimensional photonic bandgap cavities determined by the finite-element method and by use of the anisotropic perfectly matched layer boundary condition," *J. Opt. Soc. Amer. B.*, Vol. 15, 2316–2324, Aug. 1998.

8. Dibben, D. C. and R. Metaxas, "Frequency domain vs. time domain finite element methods for calculation of fields in multimode cavities," *IEEE Trans. Magn.*, Vol. 33, No. 2, 1468–1471, Mar. 1997.

9. Rodriguez-Esquerre, V. F., M. Koshiba, and H. E. Hernandez-Figueroa, "Finite-element analysis of photonic crystal cavities: Time and frequency domain," *IEEE J. Lightw. Technol.*, Vol. 23, No. 3, 1514–1521, Mar. 2005.

10. Tayeb, G. and D. Maystre, "Rigorous theoretical study of finite-size two-dimensional photonic crystals doped by microcavities," *J. Opt. Soc. Am. A*, Vol. 14, No. 12, 3323–3332, Dec. 1997.

11. Maystre, D., "Electromagnetic scattering by a set of objects: An integral method based on scattering properties," *Progress In Electromagnetic Research*, PIER 57, 55–84, 2006.

12. Maystre, D., M. Saillard, and G. Tayeb, "Special methods of wave diffraction," *E-M Waves Scattering, Approximate and Numerical Methods*, Chap. 1.5.6, 2001.

13. Painter, O., K. Srinivasan, and P. E. Barklay, "Wannier-like equation for the resonant cavity modes of locally perturbed photonic crystals," *Phys. Rev. B.*, Vol. 68, 35214, July 2003.

14. Harrington, R. F., *Time-Harmonic Electromagnetic Fields*, Chap. 5, McGraw-Hill, 1961.

15. Song, B. S., S. Noda, and T. Asano, "Ultra-high-Q photonic double hetero-structure nanocavity," *Nat. Mater.*, Vol. 4, No. 3, 207–210, 2005.

16. Asano, T., B. S. Song, and S. Noda, "Analysis of the experimental Q factors ($\sim$ 1 million) of photonic crystal nanocavities," *Opt. Express*, Vol. 14, No. 5, 1996–2002, Mar. 2006.